NEAR-FIELD MIMO CHANNEL RECONSTRUCTION VIA LIMITED GEOMETRY FEEDBACK

Shima Eslami, Bikshapathi Gouda and Antti Tölli

Centre for Wireless Communications, University of Oulu, Finland
Emails: {shima.eslami, bikshapathi.gouda, antti.tolli}@oulu.fi

ABSTRACT

Near-field MIMO channels comprising line-of-sight (LoS) dominant paths can be fully described by the angle of arrivals (AoAs) and the rotation angles of both the user equipment (UE) and base station (BS), exploiting their respective antenna geometries. The resulting geometric characterization of the high-rank channels remains independent of the antenna array placement and size at both BS and UEs. Conventional near-field channel estimation requires UE-specific uplink pilots, leading to a significant pilot overhead as the number of UEs increases. In this paper, an alternative near-field MIMO channel reconstruction approach is proposed, relying on a minimal number of downlink pilots and limited geometry (angles, antenna placement) information exchange. Based on the downlink pilots transmitted from the outermost BS antennas and the prior information about the inter-antenna distance, the UEs may estimate the AoAs and rotation angles which in turn are quantized and fed back to the BS. Simulation results illustrate that just two downlink pilots suffice to characterize the channel geometry at the UEs accurately. Furthermore, an 8-bit quantization is adequate for relaying two AoAs and a rotation angle value from the UEs to the BS for full near-field LoS MIMO channel reconstruction given the known antenna placement.

Index Terms— downlink pilots, limited geometry, near-field channel reconstruction, UE-feedback.

1. INTRODUCTION

Communication in higher carrier frequencies has enabled the exploitation of antenna arrays with a large number of elements in near-field conditions where the Fraunhofer distance becomes comparable to the array size [1]. The large antenna arrays, commonly deployed at the base station (BS), and the spherical shaping of the wavefront in the near-field region provide the opportunity for focusing the transmitted/received power to a point in space given channel state information (CSI) with sufficient accuracy is available [2]. Near-field channels have unique properties in line-of-sight (LoS) settings and can be ideally represented and estimated in terms of a few geometrical parameters (such as antenna-specific distances and angles) [3–5]. In [3, 6–8], the geometry-aided near-field channel estimation is carried out by dividing the multi-input multi-output (MIMO) channel into several subchannels for which the far-field condition is assumed to be satisfied. For example, in [3, 6, 7] a short-range LoS MIMO channel is estimated using subchannel-specific likelihood functions obtained by a geometry-based message passing algorithm. Alternatively, the channel can be directly modeled with near-field array response vectors and antenna-specific geometric parameters [5, 9–13]. For instance, in [11–13] the LoS and Non-LoS (NLos) components

This work is supported by the Academy of Finland under grant no. 346208 (6G Flagship) and 343586 (CAMAIDE)

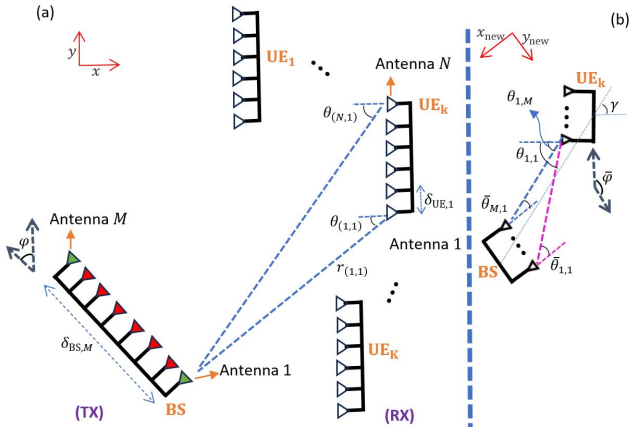

Fig. 1: A near-field LoS MIMO setup with $N_{\text{BS}} = 8$, $N = 6$, (a): with UE-specific angles, (b): with BS-specific angles.

are recovered using compressed sensing-based approaches by exploiting the polar domain sparsity. In [5, 14] the LoS channel is first represented based on a few geometric parameters and then reconstructed through a parameter estimation problem (e.g., maximum likelihood). All aforementioned studies rely on near-field parameter estimation from dedicated uplink pilots per user equipment (UE). As a result, the pilot overhead increases significantly as the number of users increases. Moreover, uplink-based channel estimation ideally requires full channel reciprocity and calibration of RF parts.

In this paper, we propose an alternative near-field LoS channel estimation scheme relying on a minimal number of downlink pilots and limited geometry information exchange. We consider a multiuser setup shown in Fig. 1-(a) where the near-field channel is fully characterized using only two pilots broadcasted from two outermost BS antennas and known antenna geometry at the transceivers. Consequently, the pilot overhead does not scale with the number of UEs. Assuming linear antenna arrays at all nodes, each UE leverages the prior information about its internal antenna placement $\{\delta_{\text{UE},i}\}_{i=1}^{N}$, shown in Fig. 1-(a), along with the known physical distance between the two active BS antennas $\delta_{\text{BS},M}$ (that is broadcasted by the BS through a control channel beforehand), to perform joint maximum likelihood (ML) estimation of three channel parameters, i.e., two angles of arrival (AoAs), i.e. $(\theta_{1,1}, \theta_{N,1})$ and the BS rotation angle ϕ. In contrast to traditional downlink-based channel estimation, each UE provides feedback of three estimated geometric parameters rather than the entire channel, using either in-band or out-of-band signaling. Finally, the BS reconstructs the channels by exploiting the prior information about the antenna placement at both BS and UEs. Numerical experiments demonstrate that just two downlink pilots combined with the prior information about the distance between BS reference antennas suffice to accurately estimate the channel parameters at the UEs.

Additionally, for a fixed number of quantization bits, converting the downlink channel parameters to the equivalent uplink ones before quantization can enhance channel estimation accuracy, given that the length of the BS is greater than that of the UEs.

2. SYSTEM MODEL

A multi-UE scenario shown in Fig. 1-(a) is considered, where a BS serves K UEs in the downlink. The BS comprises a linear antenna array with M arbitrarily spaced antenna elements, while each UE features a linear array with N arbitrarily spaced antenna elements. Moreover, both the BS and the UEs are assumed to have a fully digital architecture. The aim is to reconstruct the near-field channels $\{\mathbf{H}_k\}_{k=1}^{K}$ at the BS based on the estimated channel parameters obtained from the UEs. Since each UE computes the channel parameters independently of the others, the UE index is omitted in subsequent sections and the model is presented for an arbitrary UE. Also, We consider a carrier frequency in the millimeter-wave range, where the NLoS components can be neglected due to the significant path loss caused by the scatterers [15]. Thus $\mathbf{H} \in \mathbb{C}^{N\times M}$ denotes the LoS MIMO channel between an arbitrary UE and the BS. The $(i,j)^{\text{th}}$ entry of $\mathbf{H}$ is given by

$$\mathbf{H}(i,j) = \frac{\lambda}{4\pi r_{i,j}}\, exp\left(\frac{-\mathrm{j}2\pi r_{i,j}}{\lambda}\right), \tag{1}$$

where λ is the carrier wavelength, and $r_{i,j}$ is the distance between the j^{th} TX (BS) antenna and the i^{th} RX (UE) antenna. It is evident that the near-field LoS MIMO channel depends on antenna-specific distances. In the following sections, we will demonstrate that the distances between all the TX and RX antennas can be effectively represented by just a few (three) geometric parameters. Consequently, the near-field channel can be entirely modeled using these three geometric parameters, which remain independent of the array size and the number of antenna elements at both the TX and RX sides.

2.1. Near-Field Channel Parameters

Let $\theta_{i,j}$ denote the angle formed by the ray between the j^{th} TX (e.g., BS in downlink direction) antenna and the i^{th} RX (e.g., UE in downlink direction) antenna. Taking the first TX antenna as the reference antenna, we define the angles $(\theta_{1,1}, \theta_{N,1})$ shown in Fig. 1-(a) as two reference AoAs. Given the known antenna element spacing at the RX, we can calculate the distance from the reference antenna to all RX antennas as a function of the reference AoAs, as follows

$$r_{i,1} = \sqrt{\left(r_{1,1}\cos\theta_{1,1}\right)^2 + \left(\delta_{\text{RX},i} - r_{1,1}\sin\theta_{1,1}\right)^2}, \tag{2}$$

where $\delta_{\text{RX},i}$ is the spacing between the first and the i^{th} antennas at the RX array, and $r_{1,1}$ is given as

$$r_{1,1} = \frac{\delta_{\text{RX},N}}{\sin\theta_{1,1} - (\tan\theta_{N,1})(\cos\theta_{1,1})}, \tag{3}$$

Additionally, the distances between all other TX-RX antenna pairs can be computed as follows:

$$r_{i,j} = \sqrt{r_{i,1}^2 + (\delta_{\text{TX},j})^2 + 2\delta_{\text{TX},j}\, r_{i,1}\cos(\theta_{i,1} + \phi - \frac{\pi}{2})}, \tag{4}$$

where ϕ is the rotation angle of the TX array with respect to the direction of the RX array, $\delta_{\text{TX},j}$ stands for the spacing between the first and the j^{th} antennas at the TX array, and $\theta_{i,1}$ is given as

$$\theta_{i,1} = \tan^{-1}\left(\frac{r_{1,1}\sin\theta_{1,1} - \delta_{\text{RX},i}}{r_{1,1}\cos\theta_{1,1}}\right). \tag{5}$$

By observing (2)-(5), we can deduce that the RX can determine the location of the first TX antenna by finding the intersection of two reference AoAs, i.e., $(\theta_{1,1}, \theta_{N,1})$, provided the RX antenna spacing $(\delta_{\text{RX},i})$ are known in advance. Furthermore, the positions of the remaining TX antennas can be calculated using the location of the first TX antenna, the TX rotation angle (ϕ), and the known TX antenna spacing $(\delta_{\text{TX},j})$. Therefore, only three parameters, namely $(\theta_{1,1}, \theta_{N,1}, \phi)$, are sufficient to fully characterize the near-field LoS MIMO channels.

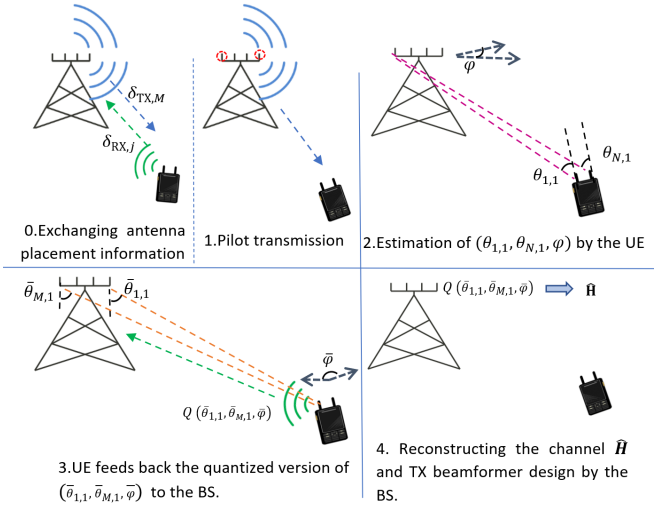

Fig. 2: Near-field DL channel reconstruction procedure

3. DOWNLINK-BASED NEAR-FIELD MIMO CHANNEL ESTIMATION

As illustrated in Fig. 2, before initiating the channel estimation process, the BS broadcasts the spacing information between its outermost antennas, denoted as $\delta_{\text{TX},M}$, to the UEs via a suitable control channel. In a similar fashion, all the UEs communicate their antenna spacing parameters, represented as $\{\delta_{\text{RX},i}\}_{i=1}^{N}$, to the BS.

Following the completion of the pilot transmission phase, each UE employs maximum likelihood estimation to determine the near-field LoS MIMO channel parameters, specifically $(\theta_{1,1}, \theta_{N,1}, \phi)$. Subsequently, these estimated parameters undergo quantization and are then transmitted back to the BS. Finally, utilizing the received parameters, the BS reconstructs the LoS MIMO channel as detailed in the following.

3.1. Near-Field Channel Parameter Estimation at Each UE

Let us denote $\mathbf{Q} \in \mathbb{C}^{2\times\tau}$ as the pilot matrix, where $\mathbf{Q}\mathbf{Q}^{\text{H}} = \tau\mathbf{I}_2$, and this matrix is transmitted from the two outermost (first and M^{th}) BS antennas. The corresponding received signal at the UE is given as

$$\mathbf{Z} \triangleq [\mathbf{H}(:,1), \mathbf{H}(:,M)]\mathbf{Q} + \mathbf{W} \in \mathbb{C}^{N\times\tau}, \tag{6}$$

where $\mathbf{W} \sim \mathcal{CN}(\mathbf{0}, \sigma^2\mathbf{I}_N)$. Each UE then correlates the received signal with the known pilot matrix to extract the signal transmitted

from the two BS antennas, as follows:

$$\mathbf{Y} \triangleq \frac{1}{\tau}\mathbf{Z}\mathbf{Q}^{\mathrm{H}}, \tag{7}$$

$$= [\mathbf{H}(:,1), \mathbf{H}(:,M)] + \frac{1}{\tau}\mathbf{W}\mathbf{Q}^{\mathrm{H}}. \tag{8}$$

For simplicity, we can represent the received signal at the UE for the j^{th} BS antenna as

$$\mathbf{y}_j \triangleq \mathbf{H}(:,j) + \mathbf{v}_j; \;\; j = 1, M, \tag{9}$$

where $\mathbf{v}_j \triangleq \frac{1}{\tau}\mathbf{W}\mathbf{q}(:,j) \sim \mathcal{CN}(\mathbf{0}, \sigma^2\mathbf{I}_N)$. Subsequently, we approximate each channel vector as $\mathbf{H}(:,j) \simeq \alpha_j\tilde{\mathbf{h}}_j$, where α_j is the common complex-valued scaling term from the j^{th} BS antenna to all the UE antennas, and based on the numerical results of [9] is defined to model the pathloss and compensate for the approximation mismatches, and

$$\tilde{\mathbf{h}}_j \triangleq \left[exp\left(\frac{-\mathrm{j}2\pi r_{1,j}}{\lambda}\right), \ldots, exp\left(\frac{-\mathrm{j}2\pi r_{N,j}}{\lambda}\right)\right]^{\mathrm{T}}. \tag{10}$$

With the above approximation and using the fact that $r_{i,j}$ is a function of three reference parameters $(\theta_{1,1}, \theta_{N,1}, \phi)$, we can rewrite (9) as

$$\mathbf{y}_j \approx \alpha_j\tilde{\mathbf{h}}_j(\theta_{1,1}, \theta_{N,1}, \phi) + \mathbf{v}_j; \;\; j = 1, M, \tag{11}$$

where $\mathbf{y}_j \sim \mathcal{CN}\big(\alpha_j\tilde{\mathbf{h}}_j(\theta_{1,1}, \theta_{N,1}, \phi), \sigma^2\mathbf{I}_N\big)$, for a given set of $\{\theta_{1,1}, \theta_{N,1}, \phi\}$ values. Accordingly, the correction factors α_j can be computed from the following objective function

$$\arg\min_{\alpha_j \in \mathbb{C}} \|\mathbf{y}_j - \alpha_j\,\tilde{\mathbf{h}}_j(\theta_{1,1}, \theta_{N,1}, \phi)\|^2. \tag{12}$$

Similar to [9, 10] the optimal α_j can be obtained by finding the first order stationary point of (12) with respect to α_j, which yields

$$\hat{\alpha}_j = \frac{\tilde{\mathbf{h}}_j^{\mathrm{H}}(\theta_{1,1}, \theta_{N,1}, \phi)\mathbf{y}_j}{\|\tilde{\mathbf{h}}_j(\theta_{1,1}, \theta_{N,1}, \phi)\|^2}, \quad j = 1, M. \tag{13}$$

Moreover, the ML estimation of $(\theta_{1,1}, \theta_{N,1}, \phi)$ can be carried out by jointly processing the signals received from both the first and M^{th} BS antennas and minimizing the resulting objective function as

$$(\hat{\theta}_{1,1}, \hat{\theta}_{N,1}, \hat{\phi}) = \underset{(\theta_{1,1}, \theta_{N,1}, \phi)}{\operatorname{argmin}} \sum_{j=1,M} \|\mathbf{y}_j - \hat{\alpha}_j\tilde{\mathbf{h}}_j(\theta_{1,1}, \theta_{N,1}, \phi)\|^2. \tag{14}$$

While the above objective function does not yield a closed-form solution for the optimal $(\theta_{1,1}, \theta_{N,1}, \phi)$ values, we can find them by searching over the feasible set of $(\theta_{1,1}, \theta_{N,1}, \phi)$ values. In case the UE does not have access to the partial BS geometry information (inter-antenna distance $\delta_{\text{BS},M}$), the intersection of AoAs can be found independently for both BS transmit antennas as

$$(\hat{\theta}_{1,j}, \hat{\theta}_{N,j}) = \underset{(\theta_{1,j}, \theta_{N,1})}{\operatorname{argmin}} \|\mathbf{y}_j - \hat{\alpha}_j\tilde{\mathbf{h}}_j(\theta_{1,j}, \theta_{N,j})\|^2, j = 1, M.$$

Consequently, the UE can estimate the angle ϕ based on the estimated angles and its known geometry. First, it computes the position vectors of j^{th} BS antenna $\hat{\mathbf{p}}_{\text{BS},j}$ using the intersection of angle pair $(\theta_{1,j}, \theta_{N,j})$ for $j = 1, M$ (see section **E** of [14]). Then it calculates ϕ as $\cos(\hat{\phi}) = \hat{\mathbf{p}}_{\text{BS}}.\mathbf{p}_{\text{UE}}/\|\hat{\mathbf{p}}_{\text{BS}}\|\|\mathbf{p}_{\text{UE}}\|$, where $\hat{\mathbf{p}}_{\text{BS}} = \hat{\mathbf{p}}_{\text{BS},1} - \hat{\mathbf{p}}_{\text{BS},M}$ and $\mathbf{p}_{\text{UE}}$ are the direction vector of the BS and the UE, respectively.

3.2. Parameter Feedback and Channel Reconstruction at BS

After parameter estimation, the UEs quantize each estimated angle with q bits and transmit them back to the BS using either in-band or out-of-band resources in the uplink. Since the BS is assumed to have prior knowledge of $\{\delta_{\text{TX},j}\}_{j=1}^{M}$ and $\{\delta_{\text{RX},i}\}_{i=1}^{N}$, it can calculate $\hat{r}_{i,j}$ from (4) and reconstruct the channel matrix $\hat{\mathbf{H}}$ as defined in (1) for each UE. However, the accuracy of $\hat{\mathbf{H}}$ depends on the number of bits used for quantizing $(\hat{\theta}_{1,1}, \hat{\theta}_{N,1}, \hat{\phi})$ parameters at the UE. Due to the smaller physical array size at the UE, small errors in $(\hat{\theta}_{1,1}, \hat{\theta}_{N,1})$ can lead to a large position error of the BS reference antenna. Similarly, the channel reconstruction is particularly susceptible to errors in the BS rotation parameter $\hat{\phi}$. In order to take advantage of the larger array size at the BS, and hence to improve the channel reconstruction accuracy given a fixed quantization budget (q bits) per channel parameter, the UE applies a simple change of coordinates where the reference angles in Fig. 1-(a) are converted to the corresponding BS reference angles illustrated in Fig. 1-(b). Specifically, the UE converts $(\hat{\theta}_{1,1}, \hat{\theta}_{N,1}, \hat{\phi})$ to $(\bar{\theta}_{1,1}, \bar{\theta}_{M,1}, \bar{\phi})$ before quantization (see Fig. 1-(b)), as follows:

$$\bar{\theta}_{i,1} = \begin{cases} \hat{\phi} + \hat{\theta}_{1,(M-i+1)} - \pi, & \text{if } \phi + \hat{\theta}_{1,(M-i+1)} \geq \pi/2 \\ \hat{\phi} + \hat{\theta}_{1,(M-i+1)}, & \text{otherwise} \end{cases}, \tag{15}$$

where $i = 1, M$ and

$$\hat{\theta}_{1,M} = \sin^{-1}\Big(\frac{\hat{r}_{1,1}\sin\hat{\theta}_{11} - \delta_{\text{BS},M}\sin(\hat{\phi} - \pi/2)}{\hat{r}_{1,M}}\Big). \tag{16}$$

Similarly,

$$\bar{\phi} = \begin{cases} \pi - \hat{\phi}, & \text{if } 0 < \hat{\gamma} + \hat{\phi} < \pi/2 \\ -\hat{\phi}, & \text{otherwise,} \end{cases}, \tag{17}$$

where $\hat{\theta}_{ij} \in [-\pi/2, \pi/2]$ and $\hat{\phi} \in [0, \pi]$ (similar equations can be provided for $\hat{\phi} \in [-2\pi, 2\pi]$) . Also, $\hat{\gamma}$ is the orientation of the BS relative to the normal of the UE array and is computed at the UE considering the coordination of Fig. 2-(a), as

$$\hat{\gamma} = \tan^{-1}\left(\frac{2\,\hat{r}_{1,1}\sin\hat{\theta}_{1,1} + \delta_{\text{BS},M}\;\cos\hat{\phi} - \delta_{\text{UE},N}}{2\,\hat{r}_{1,1}\cos\hat{\theta}_{1,1} + \delta_{\text{BS},M}\;\sin\hat{\phi}}\right). \tag{18}$$

The converted angles are quantized with q bits each and sent back to the BS as feedback. The complete procedure for near-field channel parameter estimation and reconstruction is summarized in Algorithm. 1.

Algorithm 1 Near-field channel estimation based on UE-feedback.

Data: Pilot matrix $\mathbf{Q}$, antenna-spacing at the BS and UE, i.e., $\{\delta_{\text{TX},j}\}_{j=1}^{M}$ and $\{\delta_{\text{RX},i}\}_{i=1}^{N}$, respectively.

(S.0) BS broadcasts $\delta_{\text{TX},M}$ info, while each UE provides $\{\delta_{\text{RX},i}\}_{i=1}^{N}$ to BS through UL control channels.

(S.1) **DL:** BS broadcast the pilot matrix from two antennas and each UE receives the corresponding signal as in (6).

(S.2) UE computes the near-field LoS channel parameters $(\hat{\theta}_{1,1}, \hat{\theta}_{N,1}, \hat{\phi})$ by optimizing (14) over a feasible set.

(S.3) **UL:** Each UE feedback the converted and quantized channel parameters $(\bar{\theta}_{1,1}, \bar{\theta}_{M,1}, \bar{\phi})$ to the BS.

(S.4) BS computes $\{\{r_{i,j}\}_{i=1}^{M}\}_{j=1}^{N}$ as in (4) from the received parameters and considering the UE as the TX. Then, it reconstructs the channel as in (1).

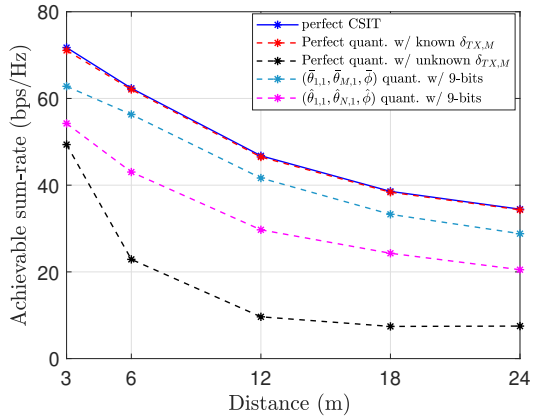

Fig. 3: Sum rate comparison with 10dB SNR for pilot transmission.

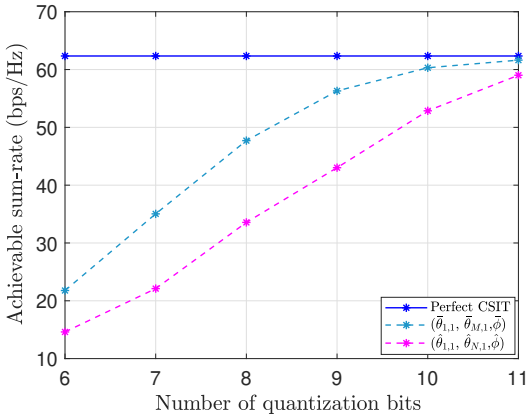

Fig. 4: Impact of the number of quantization bits for feedback at $d = 6$m.

4. NUMERICAL RESULTS

The performance of the proposed method is evaluated in a scenario where a BS comprised of a uniform linear array with $M = 32$ antennas serves $K = 2$ UEs, each equipped with a uniform linear array of $N = 16$ elements. The lengths of the arrays are set to $\delta_{\text{TX},M} = 100$ cm for the BS and $\delta_{\text{RX},N} = 16$ cm for all UEs. This setup can be likened to a large auditorium where the BS antennas are distributed along the ceiling line, and users are randomly positioned throughout the room. In addition, a pilot length of $\tau = 2$ is assumed with a received signal-to-noise ratio (SNR) of 10dB. The wavelength (λ) is assumed to be 5 mm, corresponding to a carrier frequency of 60 GHz. Our simulation results are based on averaging over 100 channel realizations, where for each realization, the UE positions and rotations $(\theta_{1,1}, \theta_{N,1}, \phi)$ are randomly selected from the feasible set.

To assess the accuracy of the reconstructed channels, we evaluate the achievable sum rate across users calculated as $R_{\text{sum}} = \sum_{k,l} \log(\epsilon_{k,l}^{-1})$, where $\epsilon_{k,l}$ represents the mean square error (MSE) of the l^{th} stream of the k^{th} UE at the output of the minimum MSE (MMSE) receiver. The MSE metric is computed as in [16, Eq. (5)] for a given precoder $\mathbf{m}_{k,l} \in \mathbb{C}^M$ at the BS, the MMSE combiner $\mathbf{w}_{k,l} \in \mathbb{C}^N$ at the UE, and the estimated channel $\hat{\mathbf{H}}$. In this paper, the precoders $\mathbf{m}_{k,l} \in \mathbb{C}^M$ are simply computed to minimize the sum MSE objective, under the sum power constraint[1], assuming MMSE receiver at the UE. In practice, UE can compute the MMSE receiver from the precoder downlink pilots [16, 17]. The sumMSE algorithm used in the evaluation is briefly summarized in Algorithm 2.

In Fig.3, the sum rate performance of the proposed method is evaluated as a function of the distance between the midpoint of the BS and each UE. First, it can be noticed that the prior knowledge of partial BS geometry $\delta_{\text{TX},M}$ is essential to guarantee sufficient estimation quality as the similar performance with independent reference antenna positioning (without $\delta_{\text{TX},M}$) would require significantly higher pilot transmit powers. Moreover, the proposed joint estimation method leveraging the partially known BS geometry ($\delta_{\text{TX},M}$) provides near-perfect performance with ideal feedback. Thus, only two broadcast pilot sequences to all users and feeding back only three geometric parameters from each user to the BS, the MIMO channels can be estimated with sufficient accuracy. In the case of imperfect quantization, e.g., using $q = 9$ bits per angle parameter, the BS-specific angles $(\bar{\theta}_{1,1}, \bar{\theta}_{M,1}, \bar{\phi})$ are shown to provide a superior estimation accuracy than reconstructing the channel based on UE-specific parameters $(\hat{\theta}_{1,1}, \hat{\theta}_{N,1}, \hat{\phi})$.

In Figure 4, the impact of the number of quantization bits on the accuracy of the estimated channels is analyzed. An equal number of quantization bits is used for each estimated angle parameter. Again, the use of BS-specific parameters instead UE-specific parameters gives a significant performance boost given the same quantization budget. Finally, it can be seen that 9 or 10 bits quantization of $(\bar{\theta}_{1,1}, \bar{\theta}_{M,1}, \bar{\phi})$ values provides performance very close to the case with ideal CSIT.

5. CONCLUSION

In this paper, a near-field channel estimation approach with minimal downlink pilots is proposed. Considering linear arrays with known antenna geometry at the BS and UEs, we demonstrated that only two pilots from the BS antennas are sufficient to fully characterize the near-field channel, while the pilot overhead does not scale with the number of UEs. We also showed that by broadcasting two pilots from the two outermost BS antennas and leveraging prior information about antenna spacing of two active BS and all UE antennas, each UE can accurately estimate near-field channel parameters, specifically two AoAs and the relative TX-RX rotation angle. Then, each UE provides feedback of only three geometric parameters (rather than the entire channel). Lastly, we demonstrate that for a fixed number of quantization bits, converting the UE-specific channel parameters to the BS-specific ones can enhance channel estimation accuracy, given that the length of the BS is greater than that of the UEs.

Algorithm 2 Precoder/combiner design based on sumMSE minimization.

Data: Estimated channels $\{\hat{\mathbf{H}}_k\}_{k=1}^K$, noise variance of each UE σ_k^2.

Initialization: BS initialize precoders $\mathbf{m}_{k,l}\ \forall(k,l)$ randomly and to satisfy the power constraint, and set $i = 0$.

Until a predefined termination criterion is satisfied, **do:**

(S.0) $i \leftarrow i + 1$.

(S.1) BS compute the UE combiners as follows: $\mathbf{w}_{k,l} = \left(\sum_{i=1}^{K}\sum_{j=1}^{L_i} \hat{\mathbf{H}}_k \mathbf{m}_{i,j}\mathbf{m}_{i,j}^{\text{H}} \hat{\mathbf{H}}_k^{\text{H}} + \sigma_k^2 I\right)^{-1} \hat{\mathbf{H}}_k \mathbf{m}_{k,l}$.

(S.2) BS computes the precoders as follows: $\mathbf{m}_{k,l} = \left(\sum_{i=1}^{K}\sum_{j=1}^{L_i} \hat{\mathbf{H}}_i^{\text{H}} \mathbf{w}_{i,j}\mathbf{w}_{i,j}^{\text{H}} \hat{\mathbf{H}}_i + \nu I\right)^{-1} \hat{\mathbf{H}}_k^{\text{H}} \mathbf{w}_{k,l}$. Here ν is obtained via the bisection method.

End

[1] $\min_{\mathbf{w}_{k,l}, \mathbf{m}_{k,l}} \sum_{k=1}^{K}\sum_{l=1}^{L_k} \epsilon_{k,l};\ s.t.\ \sum_{k=1}^{K}\sum_{l=1}^{L_k} \|\mathbf{m}_{k,l}\|^2 \leq 1.$

6. REFERENCES

[1] N. Deshpande, M. R. Castellanos, S. R. Khosravirad, J. Du, H. Viswanathan, and R. W. Heath, "A wideband generalization of the near-field region for extremely large phased-arrays," *IEEE Wireless Communications Letters*, vol. 12, no. 3, pp. 515–519, 2022.

[2] H. Zhang, N. Shlezinger, F. Guidi, D. Dardari, and Y. C. Eldar, "6g wireless communications: From far-field beam steering to near-field beam focusing," *IEEE Communications Magazine*, vol. 61, no. 4, pp. 72–77, 2023.

[3] J. Kaleva, N. J. Myers, A. Tölli, R. W. Heath, and U. Madhow, "Short range 3D MIMO mmwave channel reconstruction via geometry-aided AoA estimation," in *2019 IEEE 20th International Workshop on Signal Processing Advances in Wireless Communications (SPAWC)*, Nov. 2019.

[4] A. M. Elbir, K. Vijay Mishra, and S. Chatzinotas, "NBA-OMP: Near-field beam-split-aware orthogonal matching pursuit for wideband thz channel estimation," in *ICASSP 2023 - 2023 IEEE International Conference on Acoustics, Speech and Signal Processing (ICASSP)*, 2023, pp. 1–5.

[5] Y. Lu and L. Dai, "Near-field channel estimation in mixed LoS/NLoS environments for extremely large-scale mimo systems," *IEEE Transactions on Communications*, vol. 71, no. 6, pp. 3694–3707, 2023.

[6] J. Kaleva, N. J. Myers, A. Tölli, and R. W. Heath, "A geometry-aided message passing method for aoa-based short range MIMO channel estimation," in *2019 IEEE 20th International Workshop on Signal Processing Advances in Wireless Communications (SPAWC)*, 2019, pp. 1–5.

[7] N. J. Myers, J. Kaleva, A. Tölli, and R. W. Heath, "Message passing-based link configuration in short range millimeter wave systems," *IEEE Transactions on Communications*, vol. 68, no. 6, pp. 3465–3479, 2020.

[8] A. Fascista, B. J. B. Deutschmann, M. F. Keskin, T. Wilding, A. Coluccia, K. Witrisal, E. Leitinger, G. Seco-Granados, and H. Wymeersch, "Uplink joint positioning and synchronization in cell-free deployments with radio stripes," in *2023 IEEE International Conference on Communications Workshops (ICC Workshops)*, 2023, pp. 1330–1336.

[9] S. Eslami, B. Gouda, A. Tölli, and D. Kumar, "Geometry-aided joint estimation of short range mimo channels with hybrid transceivers," in *2023 IEEE International Conference on Communications Workshops (ICC Workshops)*, 2023, pp. 1204–1209.

[10] Z. Lu, Y. Han, S. Jin, M. Matthaiou, and T. Q. S. Quek, "Near-field channel reconstruction and user localization for ELAA systems," in *2022 International Symposium on Wireless Communication Systems (ISWCS)*, 2022, pp. 1–6.

[11] M. Cui and L. Dai, "Channel estimation for extremely large-scale mimo: Far-field or near-field?" *IEEE Transactions on Communications*, vol. 70, no. 4, pp. 2663–2677, 2022.

[12] X. Zhang, H. Zhang, and Y. C. Eldar, "Near-field sparse channel representation and estimation in 6G wireless communications," *arXiv preprint arXiv:2212.13527*, 2022.

[13] M. Cui and L. Dai, "Near-field wideband channel estimation for extremely large-scale MIMO," *Science China Information Sciences*, vol. 66, no. 7, p. 172303, 2023.

[14] S. Eslami, B. Gouda, A. Tölli, and D. Kumar, "Geometry-aided joint estimation of short range MIMO channels with hybrid transceivers," in *Proceedings of the International Communication Conference (ICC)*, 2023.

[15] M. Cui, L. Dai, Z. Wang, S. Zhou, and N. Ge, "Near-field rainbow: Wideband beam training for XL-MIMO," *IEEE Transactions on Wireless Communications*, vol. 22, no. 6, pp. 3899–3912, 2023.

[16] J. Kaleva, A. Tölli, and M. Juntti, "Weighted sum rate maximization for interfering broadcast channel via successive convex approximation," in *2012 IEEE Global Communications Conference (GLOBECOM)*, 2012, pp. 3838–3843.

[17] J. Kaleva, A. Tölli, and M. Juntti, "Decentralized sum rate maximization with qos constraints for interfering broadcast channel via successive convex approximation," *IEEE Transactions on Signal Processing*, vol. 64, no. 11, pp. 2788–2802, 2016.